Preliminary Neutronic Analysis Results of Accident Tolerant Fuel Loaded OPR-1000 with STREAM/RAST-K 2.0 code

Yunki Jo, Eun Jeong, Alexey Cherezov and Deokjung Lee*
Department of Nuclear Engineering, Ulsan National Institute of Science and Technology
50 UNIST-gil, Ulsan, 44919, Republic of Korea
**Corresponding author: deokjung@unist.ac.kr*

1. Introduction

Recently, there have been lots of research related with the accident tolerant fuel (ATF) to enhance the safety of nuclear power plants. Korea Atomic Energy Research Institute (KAERI) has suggested ATFs using UO_2 pellet with metallic additives such as Molybdenum (Mo) and Chromium (Cr) to increase a thermal conductivity of fuel pellet [1]. Additionally, KAERI has suggested the Cr-coated Zircaloy-4 cladding to reduce high temperature oxidation and corrosion rate [2]. The yttrium oxide (Y_2O_3) oxide-dispersion-strengthened (ODS) has also been suggested to increase a mechanical strength of fuel rod [3]. Previously, neutronic analysis of ATF loaded core has been performed by DeCART/MASTER code at Kyung Hee University [4].

In this work, the ATF model containing UO_2-5 vol% Mo microcell (UO_2-5Mo), Y_2O_3 ODS and CrAl coating is applied to PLUS7 fuel assembly. Reactor design of ATF core is performed based on OPR-1000 model, and STREAM/RAST-K 2.0 (ST/R2) two-step scheme is used for the core calculation. Detail specification of the ATF model is given in Section 2. The main objective of this work is presenting preliminary neutronic analysis results about feasibility of ATF loaded core in a neutronics perspective.

2. Methods and Results

2.1 Computational codes

Two-step scheme with ST/R2 codes is used for ATF loaded core calculations. STREAM is a lattice physics code using the method of characteristics (MOC). STREAM generates homogenized few group macroscopic cross section data of fuel assemblies for RAST-K 2.0. In STREAM, it is possible to treat resonance effect of Mo nuclides by using the pin-based point-wise energy slowing down method (PSM). In the previous work, the effect of resonance treatment for Mo nuclides in ATF was analyzed [5]. The resonance treatment of Mo nuclides in ATF loaded PLUS7 type assembly caused 700–1200 pcm decrease in multiplication factor depending on its burnup. RAST-K 2.0 is a three-dimensional nodal diffusion code. A core calculation is performed with RAST-K 2.0 by using the few group macroscopic cross section data generated by STREAM. In RAST-K 2.0, it is possible to use fuel assembly-wise thermal conductivity for conventional UO_2 fuel and ATF [6].

2.2 Accident tolerant fuel model

Fig. 1 shows the configuration of UO_2 pin and ATF pin. UO_2-5Mo is used as a fuel in the ATF pin. It means that the ATF pin contains less fuel amount of 95% compared to UO_2 pin. Additionally, Mo metallic additive has a high resonance cross section. These characteristics of ATF pin causes shorter cycle length of ATF loaded core. In ATF pins, the outermost ZIRLO layer of 80 microns is replaced by Y_2O_3 ODS, and it is coated with CrAl alloy of 20 microns. In the previous work, it is observed that the Y_2O_3 ODS and CrAl coating have a minor effect in neutronics perspective [6]. The detail specifications of UO_2 and ATF pins are shown in Table I.

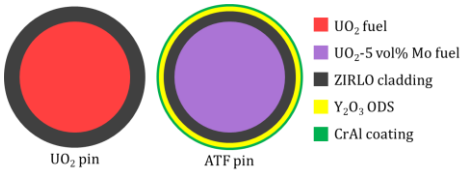

Fig. 1. Configuration of UO_2 pin and ATF pin

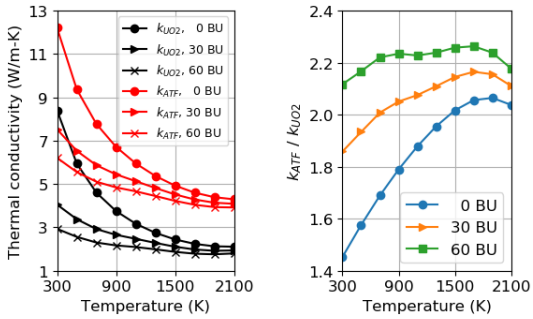

Fig. 2. Thermal conductivity of UO_2 and UO_2-5 vol% Mo microcell. Burnup is in GWd/MTU.

Fig. 2 shows the thermal conductivity of UO_2 (k_{UO2}) and UO_2-5Mo (k_{ATF}). k_{UO2} is calculated by the modified Nuclear Fuel Industries (NFI) thermal conductivity model that is used in FRAPCON-4.0 [7]. k_{ATF} is calculated by using the effective thermal conductivity equation for heterogeneous materials with co-continuous phases [8]. k_{ATF} is 1.5–2.3 times higher than k_{UO2} due to high thermal conductivity of Mo.

2.3 Reactor core model

OPR-1000 reactor core is used for reactor analysis of

ATF loaded core. It is assumed that ATF is loaded from a specific cycle of UO_2 core, not the 1st cycle. From the cycle that ATF started to be loaded, the same loading pattern (LP) of each case was repeatedly used to find an equilibrium core.

Table I: Test case description

Case	UO2	ATF-0	ATF-1	ATF-2
Fuel pin and assembly information				
Fuel type	UO_2	UO_2-5 vol% Mo	UO_2-5 vol% Mo	UO_2-5 vol% Mo
Enrichment (wt%) (normal/zoning)	4.5/4.0	4.5/4.0	4.9/4.4	4.5/-
Pellet density (g/cm^3)	10.313	10.28085	10.28085	10.28085
Pellet radius (cm)	0.4095	0.4095	0.4095	0.4095
ZIRLO cladding thickness (cm)	0.057	0.049	0.049	0.049
Y_2O_3 ODS thickness (cm)	-	0.008	0.008	0.008
CrAl coating thickness (cm)	-	0.002	0.002	0.002
Fuel rod radius (cm)	0.4750	0.4770	0.4770	0.4770
# of zoned fuel pins in FA	52	52	52	0
Core information				
Loading pattern	Fig. 3	Fig. 3	Fig. 3	Fig. 4
# of fresh FA	69	69	69	69
# of fresh BP rods	816	816	816	340

Table I shows the test cases used in this work. UO2 case represents the conventional UO_2 core. ATF cases, which are ATF-0, ATF-1 and ATF-2, represent the ATF loaded core. In ATF cases, ATF pin model shown in Fig. 1 is used instead of UO_2 pin except axial blanket region and BP rod positions where 2 wt% UO_2 fuel is used. ATF-0 case and ATF-1 case use the same LP of UO2 case shown in Fig. 3. ATF-0 case is set to show the effect of using ATF pins instead of UO_2 pins. In ATF-1 case, the enrichments of normal and zoned fuel pins are increased to 4.9 and 4.4 wt%, respectively, to compensate the reduced amount of fissile material in ATF pins. In ATF-2 case, every zoned fuel rod is replaced by the normal enriched fuel rod, and the number of fresh burnable poison (BP) rods are largely reduced to increase the amount of fuels in the core. There are only 340 fresh gadolinia fuel rods in the core of ATF-2 case, while there are total 816 fresh gadolinia fuel rods in the core of UO2. The LP shown in Fig. 4 is used for ATF-2 case instead of the one used in UO2 case. Table II shows the design limit used in this work for ATF loaded OPR-1000.

Table II: Design limit for ATF loaded OPR-1000

Design parameter	Design limit
F_q, 3-D peaking factor	< 2.578
F_r, 2-D peaking factor	< 1.6
Max. pin burnup	< 60 GWD/MTU
MTC at BOC, HZP, ARO, No Xe	< 9 pcm/K
MTC at BOC, HFP, ARO, Eq. Xe	< 0 pcm/K
MTC at EOC, HFP, ARO, Eq. Xe	< 0 pcm/K > -72 pcm/K

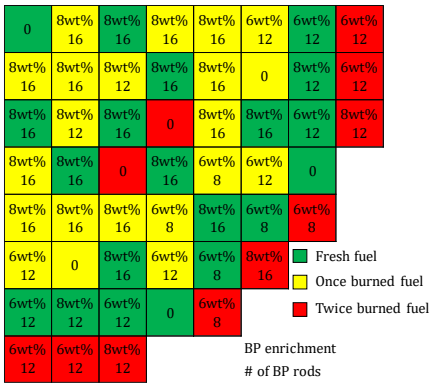

Fig. 3. Loading pattern of UO2, ATF-0 and ATF-1 cases

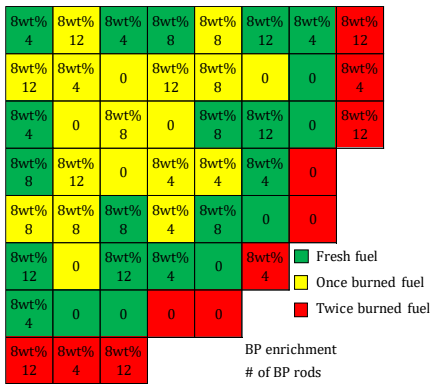

Fig. 4. Loading pattern of ATF-2 case

2.3 Numerical results of equilibrium core

This section presents numerical results of equilibrium core of test cases. Table III shows the summary of design limit parameters. All four test cases satisfied the design limit shown in Table II. Cycle length of ATF-0 case is 64 EFPDs shorter than UO2 case. As it is mentioned in the previous section, it is due to less fuel loading and more absorber material of Mo in the core. By increasing fuel enrichment, the cycle length of ATF-1 case is increased by 41.7 EFPDs compared with ATF-0 case. However, it is still 22.3 EFPDs shorter than UO2 case.

Table III: Summary of design limit parameters

Case	UO2	ATF-0	ATF-1	ATF-2
Cycle length (EFPD)	472.1	408.1	449.8	435.5
Max. F_q	1.881	1.910	1.946	2.151
Max. F_r	1.480	1.499	1.507	1.594
Max. pin burnup (GWD/MTU)	59.274	53.835	58.814	57.227
MTC at BOC, HZP, ARO, No Xe (pcm/K)	4.96	-1.17	0.83	7.30
MTC at BOC, HFP, ARO, Eq. Xe (pcm/K)	-19.04	-24.69	-21.77	-13.14
MTC at EOC, HFP, ARO, Eq. Xe (pcm/K)	-68.01	-67.39	-69.20	-69.74

In ATF-2 case, although there is no increase of fuel enrichment, the cycle length is increased by 27.4 EFPDs compared with ATF-0 case. It is the combined effect of

replacing zoned fuel rods with normal fuel rods, reducing the number of fresh BP rods and using different LP.

Fig. 5 shows the critical boron concentration (CBC) results. During the burnup cycle, the CBC of ATF-0 case is lower than the one of UO2 case due less amount of fuel and more neutron absorption by Mo. While CBC of ATF-1 case is in a similar level with UO2 case at beginning of cycle (BOC), it decreases more steeply as burnup increases. CBC of ATF-2 case is higher than the one of UO2 case at BOC due to the smaller number of BP rods in the core.

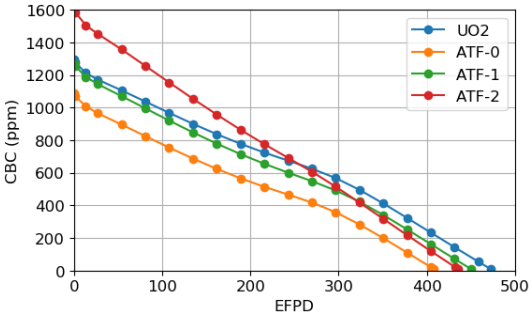

Fig. 5. Comparison of critical boron concentration

Fig. 6 shows the moderator temperature coefficients (MTC) results. MTC results show the same tendency with the CBC results shown in Fig. 5. MTC is mainly affected by the boron concentration in moderator. During the burnup cycle, MTC of ATF-0 and ATF-1 cases are more negative than MTC of UO2 case due to lower CBC of them. On the other hand, at BOC, MTC of ATF-2 case is less negative than MTC of UO2 case due to much higher CBC shown in Fig. 5.

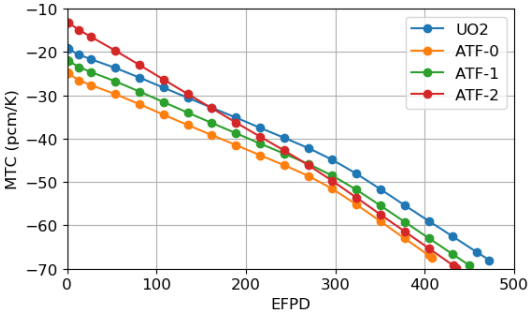

Fig. 6. Comparison of moderator temperature coefficients

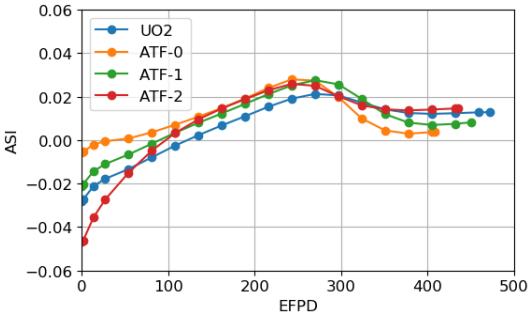

Fig. 7. Comparison of axial shape index

Fig. 7 shows the axial shape index (ASI) results. At BOC, axial powers of ATF-0 and ATF-1 cases are slightly more bottom skewed than UO2 case, while the one of ATF-2 case is more top skewed. It is due to the less negative MTC of ATF-2 case shown in Fig. 6. When MTC is more negative, reactor power at the top half of core is more decreased due to larger negative feedback.

Fig. 8 shows the peaking factor results. At BOC, F_q and F_r of ATF-2 case is much higher than the ones of the other cases due to smaller number of BP rods in the core. F_q and F_r values of four test cases still satisfy the design limits shown in Table II.

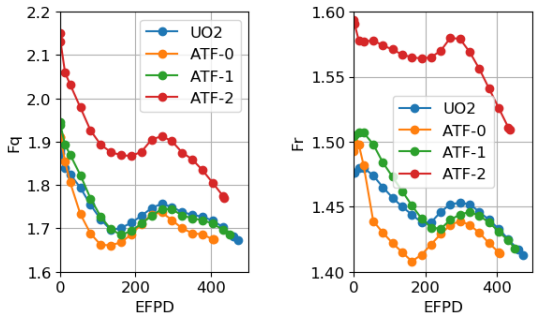

Fig. 8. Comparison of peaking factors, F_q and F_r

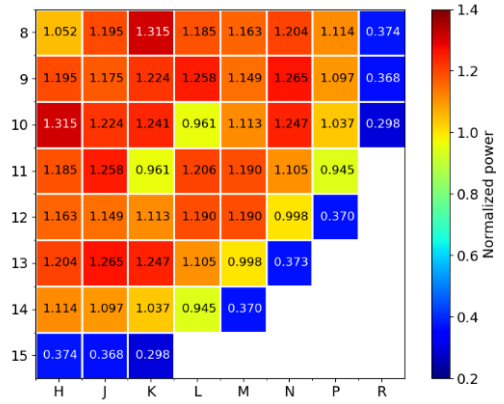

Fig. 9. Radial power distribution of UO2 case at BOC

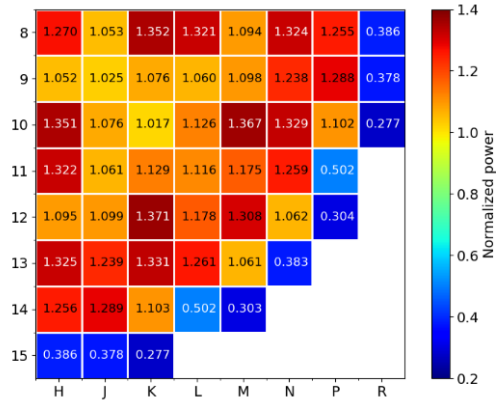

Fig. 10. Radial power distribution of ATF-2 case at BOC

Fig. 9 and Fig. 10 show the fuel assembly-wise radial power distribution of UO2 and ATF-2 cases at BOC,

respectively. The radial power distributions of ATF-0 and ATF-1 cases are omitted, because they are similar with UO2 case shown in Fig. 10. The radial power distribution of UO2 case is flatter than ATF-2 case due to the larger number of BP rods helping to reduce local peak power. However, it should be noted that the reduction of BP rods in ATF-2 case is possible due to additional neutron absorber, Mo, in ATF.

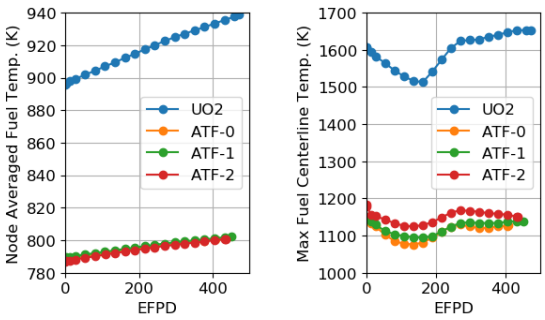

Fig. 11. Comparison of fuel temperature

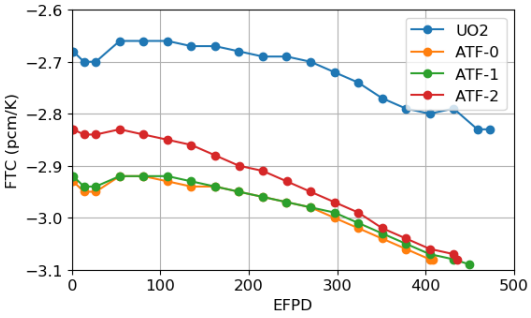

Fig. 12. Comparison of fuel temperature coefficients

Fig. 11 shows the maximum fuel centerline temperature. The maximum fuel centerline temperatures of ATF cases are 400–500 K lower than the one of UO2 case due to higher thermal conductivity of UO_2-5Mo shown in Fig. 2. Fig. 12 shows the comparison of fuel temperature coefficients (FTC). FTC of ATF cases are more negative than UO2 case due to its lower fuel temperature shown in Fig. 11 and metallic additive of Mo having high resonance cross section. FTC of ATF-2 case is less negative than FTC of ATF-0 and ATF-1 cases. It is caused by the less amount of BP material, gadolinia, in the core.

3. Conclusions

In this work, a reactor analysis of ATF loaded cores has been performed with ST/R2. Based on OPR-1000 core model, the results of ATF cores are compared with the UO_2 core results. Cycle lengths of ATF cases are shorter than the one of UO2 case due to the less amount of fuel and high resonance cross section of Mo metallic additive in ATF. Cycle length of ATF-0 case is 64 EFPDs shorter than UO2 case. By increasing U-235 enrichment by 0.5 wt%, the cycle length of ATF-1 case is increased by 41.7 EFPDs compared with the ATF-0 case. On the other hand, cycle length of ATF-2 case is increased by 27.4 EFPDs compared with ATF-0 case by replacing zoned fuel rods with normal fuel rods and changing LP of the core. It should be noted that the reduction of BP rods in ATF-2 case is possible due to additional neutron absorber which is Mo metallic additive in ATF. The radial power distribution of UO2 case is flatter than the one of ATF-2 case due to the reduced number of fresh BP rods in ATF-2 case. The maximum fuel centerline temperatures of ATF cases are 400–500 K lower than the one of UO2 case. It is due to 1.5–2.3 times higher thermal conductivity of ATF compared with UO_2 fuel. The lower fuel temperature of ATF caused more negative FTC. For the future work, rod ejection accident analysis and economic evaluation for ATF loaded core will be performed.

ACKNOWLEDGEMENTS

This work has been carried out under the Nuclear R&D Program supported by the Ministry of Science and ICT. (NRF-2020M2A8A5025118)

REFERENCES

[1] D. J. Kim, K. S. Kim, D. S. Kim, J. S. Oh, J. H. Kim, J. H. Yang, and Y. H. Koo, Development Status of Microcell UO_2 Pellet for Accident-tolerant fuel, *Nucl. Eng. Technol.*, **Vol. 50**, p. 253-258, 2018.
[2] H. G. Kim, I. H. Kim, Y. I. Jung, D. J. Park, J. Y. Park, and Y. H. Koo, Adhension Property and High-temperature Oxidation Behavior of Cr-coated Zircaloy-4 Cladding Tube Prepared by 3D Laser Coating, Journal of Nuclear Materials, Vol. 465, p. 531-539, 2015.
[3] Y. Jung, H. Kim, H. Guim, Y. Lim, J. Park, D. Park, and J. Yang, Surface treatment to form a dispersed Y_2O_3 layer on Zircaloy-4 Tubes, *Applied Surface Science*, **Vol. 429**, p. 272-277, 2018.
[4] D. H. Hwang, S. G. Hong, and W. K. In, Physical Characteristics of a PWR Core Loaded with Micro-cell UO2 Pellet Fuels, *Ann. Nucl. Energy*, **Vol. 128**, p. 33-43, 2019.
[5] E. Jeong, Y. Jo, S. Choi, H. Lee, H. C. Shin, K. Lee, and D. Lee, Neutronics Effect to Reactor Core Analysis of Molybdenum Micro-cell Type Accident Tolerance Fuel, *Transactions of the Korean Nuclear Society Spring Meeting*, Jeju, Korea, May 23-24, 2019.
[6] E. Jeong, Y. Jo, S. Choi, H. Lee, H. C. Shin, K. Lee, and D. Lee, Accident Tolerant Fuel Neutronics Analysis for Commercial PWR using Metallic Micro-cell UO2-Mo (or Cr) Pellets with Cr-based Cladding Coating, *Transactions of the Korean Nuclear Society Spring Meeting*, Goyang, Korea, October 24-25, 2019.
[7] KJ Geelhood, WG Luscher, PA Raynaud, IE Porter, FRAPCON-4.0: A Computer Code for the Calculation of Steady-State, Thermal-Mechanical Behavior of Oxide Fuel Rods for High Burnup, PNNL-19418, **Vol. 1**, 2015.
[8] J. Wang, J. K. Carson, M. F. North, and D. J. Cleland, A New Structural Model of Effective Thermal Conductivity for Heterogeneous Materials with Co-continuous Phases, *International Journal of Heat and Mass Transfer*, **Vol. 51**, p. 2389-2397, 2008.